Total Cross Sections for Ionization and Attachment in Gases by Electron Impact. I. Positive Ionization

Donald Rapp, and Paula Englander-Golden

Citation: The Journal of Chemical Physics **43**, 1464 (1965); doi: 10.1063/1.1696957
View online: http://dx.doi.org/10.1063/1.1696957
View Table of Contents: http://aip.scitation.org/toc/jcp/43/5
Published by the American Institute of Physics

kinematic theory for the description of fast electron scattering from small atoms. The comparison of the electron-scattering results with the x-ray results given in Sec. 3 indicates that the first-order theories for the inelastic term $ZS(s)$ are complementary in the sense that errors in the x-ray expression are minimized for small scattering angles while the reverse is true for the electron-scattering case.

Note added in proof: Infinities in the limit as s goes to zero in the total intensity expression also occur in the Morse term. This difficulty can be removed artificially by choosing s to be $s_{01}=(k^2+k_1^2-2kk_1\cos\theta)^{\frac{1}{2}}$ in that part of the intensity expression corresponding to purely inelastic scattering.

ACKNOWLEDGMENTS

The author wishes to thank Professor R. Mazo for pointing out the existence of Ref. 3, and Professor Y. Morino and Professor K. Kimura for their helpful discussions and for their kind hospitality. Thanks are also due Professor L. S. Bartell and Dr. D. A. Liberman for reading the manuscript and for making several helpful suggestions.

THE JOURNAL OF CHEMICAL PHYSICS VOLUME 43, NUMBER 5 1 SEPTEMBER 1965

Total Cross Sections for Ionization and Attachment in Gases by Electron Impact. I. Positive Ionization

DONALD RAPP AND PAULA ENGLANDER-GOLDEN
Lockheed Missiles and Space Company, Palo Alto, California

(Received 21 April 1965)

The total ionization cross sections of He, Ne, Ar, Kr, Xe, H_2, D_2, N_2, O_2, CO, NO, CO_2, N_2O, and CH_4 have been measured from threshold to 1000 eV in a total ionization tube. More limited measurements were performed in C_2H_4 and SF_6. Great care was taken to assure complete collection of electron and ion currents, and the absence of spurious instrumental errors. A new method was devised for obtaining absolute cross sections of gases relative to H_2, and a McLeod gauge was used to obtain the absolute cross section in H_2. The cross sections in NO and O_2 could not be obtained by this method, and an approximate correction to direct McLeod-gauge readings was used for these gases. It is believed that the results are as accurate as is possible with the present method. It is difficult to explain the differences found between cross sections measured by various investigators. McLeod-gauge errors appear to account for most of the difference in absolute magnitude.

I. INTRODUCTION

ONE of the most fundamental measurements in the field of electronic- and atomic-impact phenomena is the absolute total cross section for ionization of a gas by electron impact.[1–3] These cross sections play a pivotal role in normalization of modulated-beam experiments,[4–7] and are also of importance in application to plasma physics, vacuum technology, and the ionosphere.

In the early 1930's, a series of very careful experiments on ionization were performed by Smith, Tate, Bleakney, and co-workers[1,2,8–11] on ionization processes in gases by electron impact. Until recently, this work had been repeated and extended in only a very few instances.[12–15] The later work has not generally been any improvement over the earlier work, and the results of Refs. 1 and 2 have remained as the standard in this field for 30 years.

In the last few years, three separate laboratories have set about more ambitious programs for repeating and extending the work of the early total ionization cross-section measurements.[16–19] The interest in this work has led to the recent preparation of a review article on this subject.[20]

[1] P. T. Smith, Phys. Rev. **36**, 1293 (1930).
[2] J. T. Tate and P. T. Smith, Phys. Rev. **39**, 270 (1932).
[3] E. W. McDaniel, *Collision Phenomena in Ionized Gases* (John Wiley & Sons, Inc., New York, 1964), p. 174.
[4] W. L. Fite and R. T. Brackmann, Phys. Rev. **113**, 815 (1959).
[5] W. L. Fite and R. T. Brackmann, Phys. Rev. **112**, 1141 (1958).
[6] A. C. H. Smith, E. Caplinger, E. W. Rothe, and S. M. Trujillo, Phys. Rev. **127**, 1647 (1962).
[7] E. W. Rothe, L. L. Marino, R. H. Neynaber, and S. M. Trujillo, Phys. Rev. **125**, 582 (1962).
[8] P. T. Smith, Phys. Rev. **37**, 808 (1931).
[9] W. Bleakney, Phys. Rev. **35**, 139 (1930).
[10] W. Bleakney, Phys. Rev. **33**, 1180 (1930).
[11] W. Bleakney, Phys. Rev. **36**, 1303 (1930).
[12] H. Harrison, Ph.D. thesis, Catholic University of America, Washington, D. C., 1956.
[13] J. W. Liska, Phys. Rev. **46**, 169 (1934).
[14] B. A. Tozer and J. D. Craggs, J. Electron **8**, 103 (1960).
[15] F. W. Lampe, J. L. Franklin, and F. H. Field, J. Am. Chem. Soc. **79**, 6129 (1956).
[16] B. L. Schram, F. J. de Heer, M. J. van der Wiel, and J. Kistemaker, Physica **31**, 94 (1965).
[17] R. K. Asundi and M. V. Kurepa, J. Electron. Control **15**, 41 (1963).
[18] R. K. Asundi, J. D. Craggs, and M. V. Kurepa, Proc. Phys. Soc. (London) **82**, 967 (1963).
[19] D. Rapp, P. E. Golden, and D. D. Briglia, Bull. Am. Phys. Soc. **10**, 181 (1965); P. E. Golden and D. Rapp, Lockheed Missiles and Space Company Tech. Rept. 6-74-64-12, January 1964.
[20] L. J. Kieffer, "A Compilation of Critically Evaluated Electron Impact Ionization Cross Section Data for Atoms and Diatomic Molecules," Joint Institute for Laboratory Astrophysics Rept. No. 30, Boulder, Colorado, 5 February 1965.

The purpose of the present paper is to summarize our results for the total ionization cross sections of He, Ne, Ar, Kr, Xe, H_2, D_2, N_2, O_2, CO, NO, CH_4, CO_2, and N_2O over an energy range from threshold to 1000 eV. In addition, a limited amount of data were taken on SF_6 and C_2H_4.

The emphasis in the present work is on consistency checks[21] to ensure complete collection of ions and electrons, and to show that the cross sections are independent of spurious instrumental errors. Because of these results, it is believed that the energy dependence of the cross sections are highly accurate. The absolute normalization of the cross sections is a more difficult task, and the possible errors are consequently greater. A self-consistent technique for determination of absolute cross sections is described in a later section. It is believed that the results are as accurate as possible with the present method. Cross sections for dissociative attachment and ion-pair formation are also given in an accompanying paper. Rough total cross sections for dissociative ionization have been given in a previous paper.[22]

II. EXPERIMENTAL METHOD FOR POSITIVE IONS

The two ionization tubes used in this work have been described in detail in two recent papers.[21,22] In each case the apparatus was similar in principle to that used by Tate and Smith.[2] An electron beam from a differentially pumped, indirectly heated cathode is collimated by apertures and confined by a strong magnetic field (~600 G) to pass through a chamber containing gas at $\sim 5\times10^{-5}$ Torr, and then into an electron collector. The entire system was bakable, and had a base pressure of 10^{-9} Torr. A uniform electric field maintained perpendicular to the electron beam accelerates ions out of the electron beam to an ion collector. The total ionization cross section is calculated from

$$\sigma_T = i_I/i_e n l, \tag{1}$$

where i_I is the ion current, i_e is the electron current, n is the target-gas number density, and l is the effective path length of the electrons contributing to ion collection. For a gas capable of multiple ionization, the total cross section is a charge-weighted sum of partial ionization cross sections:

$$\sigma_T = \sigma_1 + 2\sigma_2 + 3\sigma_3 + \cdots, \tag{2}$$

in which σ_n is the cross section for n-fold ionization.

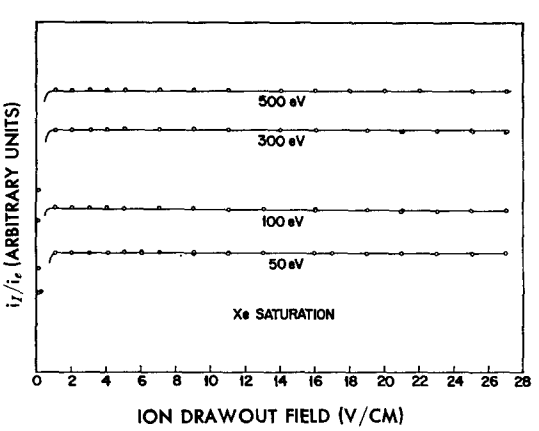

FIG. 1. Ion-current saturation curves in xenon as a function of ion drawout field, $V_{\parallel}$, in volts per centimeter, for several electron energies.

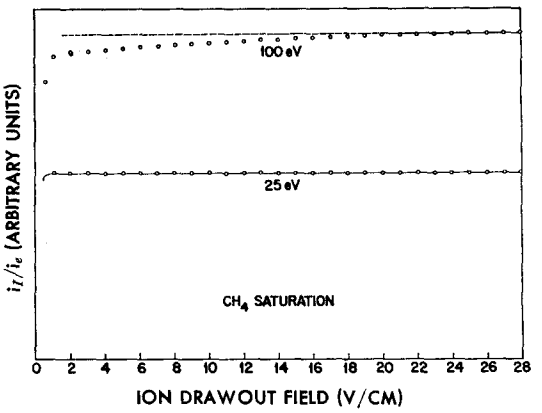

FIG. 2. Ion current saturation curves in CH_4 for 25- and 100-eV electrons. The energetic protons produced by 100-eV electrons require a much higher ion drawout field to be completely collected.

The consistency checks necessary for accurate cross sections in a total ionization tube have been mentioned in a previous paper.[21] One must show that the electron current and ion current are completely collected, that path length corrections are not important, and that space charge effects are not causing errors. Proof of complete collection of electron and ion currents is obtained by raising the respective current collecting fields until no further increase in current is observed. When the current is "saturated," it is interpreted as 100% collection. Saturation curves for electrons with energies of 28, 75, 300, and 500 eV are shown in Ref. 21. The saturation curves for positive ions are shown in Ref. 19 in detail. For atoms, an electric field of ~2–5 V/cm is sufficient to ensure complete collection of the ions formed, as shown in Fig. 1 for Xe. In molecules, however, the energetic ions formed by dissociative ionization[22] require much higher ion-collection fields. An example of this is shown in Fig. 2 for CH_4 with 100- and 25-eV electrons. At 25 eV, few energetic dissociated ions can be formed, and the ions are essentially all low-energy particles that are saturated by weak fields. At 100 eV, however, dissociative ionization results in a substantial number of very energetic protons, which require almost 30 V/cm for complete collection. In all the work done in the present experiments, a field sufficient to collect all the ions in a fixed

[21] D. D. Briglia and D. Rapp, J. Chem. Phys. **42**, 3021 (1965).
[22] D. Rapp, P. E. Golden, and D. D. Briglia, J. Chem. Phys. **42**, 4081 (1965).

TABLE I. Ion-collection field strength for complete collection of ions at ion collector.

Gas	Field strength (V/cm)
He	5
Ne	5
Ar	5
Kr	5
Xe	5
H_2, D_2	25
N_2	15
O_2	25
CO	15
NO	21
N_2O	20
CO_2	20
CH_4	26
SF_6	20
C_2H_4	26

path length was maintained. Table I gives the field strengths used.

The absence of space-charge effects was shown by the independence of the cross sections on variation of the electron current. It was also shown that above ~300 G, the cross sections were independent of magnetic field. This is evidence for the absence of electron path-length corrections, although further discussion of this point is given in a later section.

After the consistency checks described above were checked out in detail, cross sections for the various gases were measured under proper conditions of complete ion and electron collection. This was done by first measuring the energy dependence of the cross section for each gas in a series of runs on an X–Y plotter, in which the energy was plotted on the X axis, and the quotient of ion current divided by electron current[23] was plotted on the Y axis. Plots were made from threshold to higher energies on scales varying from 1 to 100 V/in. Copies of most of the original data are given in Ref. 19. For completeness, copies of the original data in Xe are shown in Figs. 3(a)–(e). The pressure was held constant in the ionization tube for a time long enough (~10 min) to record a complete plot. Frequent check points were taken to ensure that the pressure did not drift. The absolute gas pressure for these relative measurements ranged from $\sim 1\times10^{-4}$ Torr in He to $\sim 1\times10^{-5}$ Torr in Xe. Smooth curves were drawn through the data, and a tabulation of relative cross sections for each gas as a function of electron energy was prepared. The energy scale was established by plotting the electron current vs electron energy and extrapolating back to zero current. The "contact potential" so measured was subtracted from the nominal electron energy set on a power supply. Good agreement was found with well-established appearance potentials in all cases.[24]

[23] D. D. Briglia and D. Rapp, Rev. Sci. Instr. **36**, 1259 (1965).

[24] F. H. Field and J. L. Franklin, *Electron Impact Phenomena* (Academic Press Inc., New York, 1957), however, see Ref. 21 regarding the onset in H_2.

The absolute normalization of the relative data can be accomplished by measuring the absolute cross section at a particular electron energy. In our first attempt at normalization,[19] a McLeod gauge was used to establish the number density of gas in the total ionization tube. The cross sections obtained in this manner were presented in Ref. 19. The method consisted of connecting a McLeod gauge, which could be pumped out by its own ultrahigh-vacuum system, to the total ionization tube by means of a $\frac{1}{2}$-in. tube that was ~100 cm long. A cold trap immersed in a dry-ice–acetone mixture was situated about half-way between the ionization tube and the McLeod gauge proper, to prevent mercury from entering the ionization tube. It was assumed that the purely effusive-flow relation

$$P_I/P_M=(T_I/T_M)^{\frac{1}{2}} \tag{3}$$

could be used to relate the pressure in the McLeod gauge, P_M, to the pressure in the ionization tube, P_I, in terms of the accurately measured temperatures. In actual practice, the ratio (T_I/T_M) was equal to 1.17. However, the mean free path for heavy gases passing through mercury at ~2 μ (the vapor pressure at room temperature) is not large compared to the tubing diameter, and deviations from effusive flow may be substantial between the McLeod gauge and the cold trap. Thus, one should really put

$$\frac{P_I}{P_M}=\frac{P_I}{P_{CT}}\frac{P_{CT}}{P_M}=\left(\frac{T_I}{T_{CT}}\right)^{\frac{1}{2}}\left(\frac{T_{CT}}{T_M}\right)^{n}, \tag{4}$$

in which the subscripts I, M, and CT represent the ionization tube, the McLeod gauge, and the cold trap, respectively. The factor n will be less than 0.5 in the region of slip flow between the McLeod gauge and the cold trap where there is a high density of mercury.[25] Since $(T_I/T_{CT})=1.82$, and $(T_{CT}/T_M)=0.644$, substantial errors could occur in the McLeod gauge if the exponent n is substantially different from 0.50.[26] For example, if n were 0.3, one would calculate (P_I/P_M) to be 1.182 from Eq. (4), and 1.081 from Eq. (3). Thus, use of Eq. (3) would lead to an apparently low value of P_I, and thus to an apparently high cross section by 9%. In view of this possibility of error,[26] as well as other possible errors in McLeod-gauge measurements for heavy gases,[27] it was decided not to rely on the McLeod-gauge measurements, except in H_2, for which it is generally accepted that errors are small.[27] Instead, a method has been devised which compares the total ionization cross section of a gas with the total ionization of H_2, independent of McLeod-gauge measurements in other gases. This method is

[25] At pressures of ~1 Torr and higher, this exponent goes to zero.

[26] The authors are particularly indebted to D. D. Briglia for pointing this out.

[27] E. W. Rothe, J. Vac. Sci. Tech. **1**, 66 (1964); H. Ishii and K. Nakayama, Trans. Natl. Vac. Symp. 8th 1961, **1**, 519 (1962); C. Meinke and G. Reich, Vakuum-Technik **11**, 86 (1962); **12**, 79 (1963).

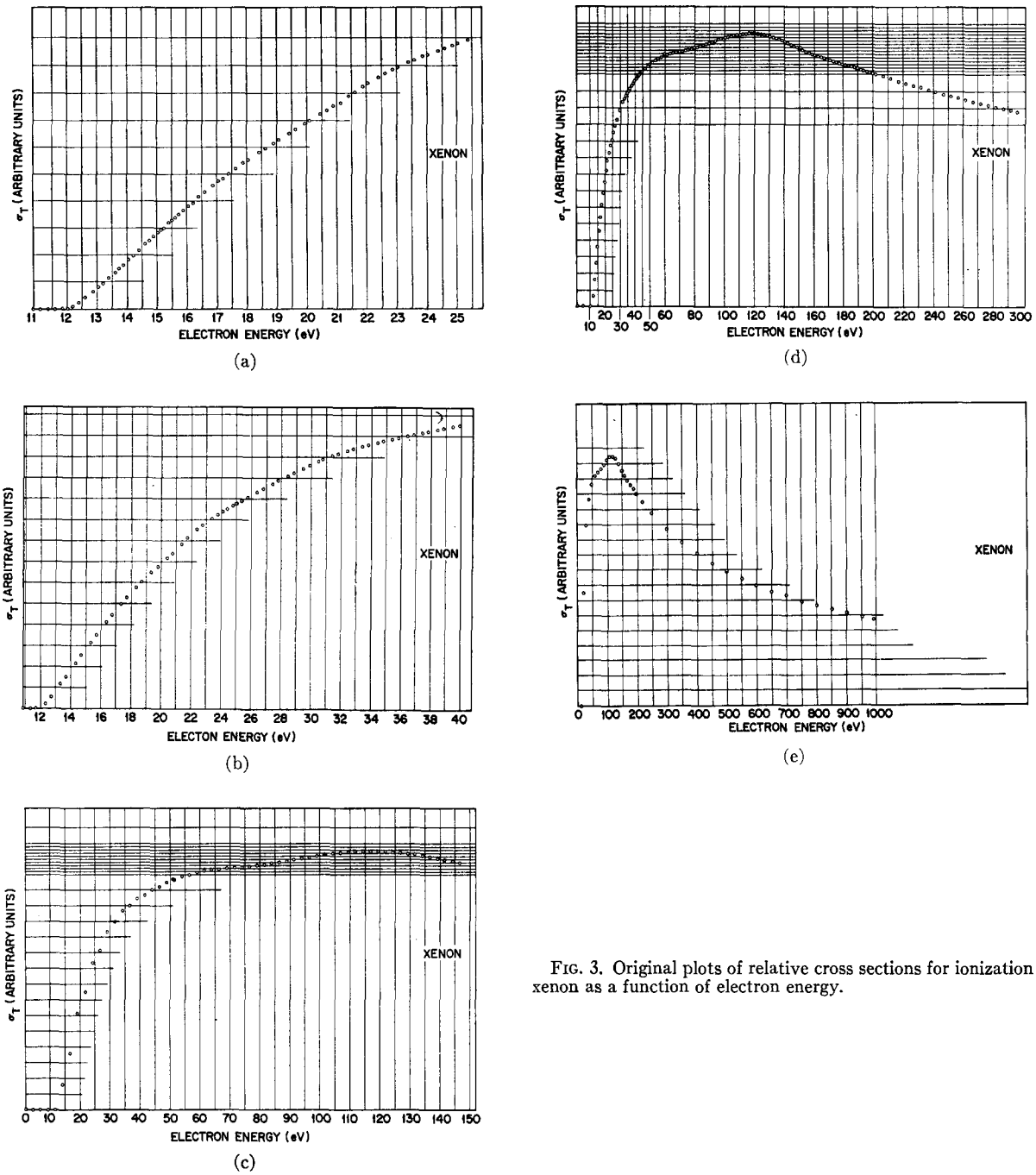

FIG. 3. Original plots of relative cross sections for ionization of xenon as a function of electron energy.

discussed in detail in the Appendix. A set of self-consistent normalization constants for the relative cross sections may then be assembled from this result. It is believed that the results of this method are more accurate than that based on direct McLeod-gauge measurements in each gas.

The perfect-gas law $n=P/RT$ was used to determine the gas density in the ionization tube. The temperature was measured by means of two thermocouples placed in the ionization tube near the ion-collector plate. The ion current was measured by means of a Cary Model 31 vibrating-reed electrometer, and the electron current was measured with a Keithley 600-A electrometer. Both electrometers were calibrated by means of a standard voltage source and standard resistors traceable to the National Bureau of Standards. The width of the ion collector determines l, and this was measured with a precise micrometer. The McLeod gauge was calibrated from the volume and capillary bore furnished by the manufacturer (Consolidated Vacuum Company, Model GM 110).

The purities of the gases used in this work were the

TABLE II. Direct data for absolute cross sections by McLeod-gauge measurements.

Gas	McLeod pressure (μ)	Temperatures (°K) McLeod	Temperatures (°K) Ionization tube	Electron current (μA)	Ion current (10^{-9} A)	Electron energy (eV)	Path length (cm)
He	0.628	298	353	0.716	0.864	116	1.83
Ne	0.436	298	353	0.810	1.456	200	1.83
	0.613			0.807	2.026		
Ar	0.175	298	353	0.754	2.35	90	1.83
Kr	0.113	298	353	0.766	2.19	85	1.83
Xe	0.149	298	353	0.792	4.85	115	1.83
H_2	0.495	298	353	0.715	1.876	68.5	1.83
D_2	0.448	298	353	0.725	1.757	70	1.83
N_2	0.149	298	353	0.844	1.895	110	1.83
O_2	0.125	298	353	0.935	1.872	125	1.83
CO	0.198	298	353	0.734	2.18	100	1.83
NO	0.139	298	353	0.911	2.35	110.5	1.83
CH_4	0.125	298	353	0.778	2.12	80	1.83
N_2O	0.104	298	353	0.863	2.07	115	1.83
CO_2	0.111	298	353	0.892	2.08	120	1.83

highest commercially available, being 99.99% or better for the rare gases, H_2, and N_2; 99.9% for O_2 and CO_2; 99.7% for CO; 99.5% for D_2; 99.0% for CH_4, C_2H_4, and NO; and 98.0% for N_2O and SF_6. Since the gases were studied at pressures $\sim 10^4$ above the residual vacuum, contamination from background impurities is negligible.

Pressures for study were kept low enough to keep multiple-scattering events below 0.5% in absolute cross sections, and 0.1% in relative cross sections.

III. EXPERIMENTAL RESULTS

The relative cross sections as functions of electron energy were obtained from plots like those shown in Figs. 3(a)–(e) for Xe. Smooth curves were drawn through the data, and a master set of tabulated relative cross sections was prepared. These cross sections were normalized by using the results of Tables II and III based on direct McLeod-gauge measurements for H_2 only. The cross sections were normalized in all other gases (except O_2 and NO) by using the results of Table IV, based on effusive-flow measurements. For O_2 and NO, the effusive-flux technique was unsatisfactory, and a rough estimate of the normalization was obtained by reducing the cross sections normalized by means of direct McLeod-gauge measurements from Table III by the average correction factor 7% found in other gases of similar constitution.

TABLE III. Calculated absolute cross sections from McLeod-gauge measurements.

Gas	$(i_I/i_e \times 10^3)$	$(T_m T_I)^{\frac{1}{2}}$ (°K)	nl (10^{13}/cm^2)	σ_T (πa_0^2)	E (eV)
He	1.207	324	3.43	0.400	116
Ne	1.798	324	2.382	0.858	200
	2.510		3.35	0.858	
Ar	3.117	324	0.956	3.71	90
Kr	2.860	324	0.618	5.26	85
Xe	6.12	324	0.814	8.54	115
H_2	2.625	324	2.705	1.103	68.5
D_2	2.422	324	2.448	1.125	70
N_2	2.254	324	0.814	3.15	110
O_2	2.002	324	0.683	3.33	125
CO	2.971	324	1.082	3.12	100
NO	2.575	324	0.760	3.85	110.5
CH_4	2.725	324	0.683	4.53	80
N_2O	2.400	324	0.586	4.80	115
CO_2	2.332	324	0.617	4.30	120

The final cross sections are tabulated in Tables V–VII for rare gases, diatomics, and polyatomics, respectively. The energy dependence of the cross sections within several volts of threshold are not easy to define exactly because the energy spread in the electron beam ($\sim$0.3 eV full width at half-height) rounds sharp corners at "breaks," and because some judgment is involved in fitting curves through the data in this region of energy. The present work was intended mainly to characterize the ionization cross sections over a broad range of energy from threshold up to 1000 eV, and discovery of possible fine structure near threshold occupied less interest in this work. However, direct plots of near-threshold cross sections are available from the author.[19] There is not space to include all these data in the present work, but several representative examples are shown in Figs. 4(a)–(d). Comprehensive plots of cross section vs electron energy for the rare gases are shown in Fig. 5 and for diatomic molecules in Fig. 6.

IV. DISCUSSION OF RESULTS

The possibility of errors in the energy dependences of the cross sections depends on errors in the measurement of $i_I/i_e nl$ as a function of electron energy. The results were taken in a flow system in which the ionization chamber was pumped on through a small hole to achieve differential pumping of the cathode. By taking frequent repeat measurements of the cross section at some fixed energy, the constancy of the number density during a run was established. Data were only retained when this constancy was better than

TABLE IV. Direct data for absolute cross sections by effusive-flow measurements.

Exptl. series	Gas	Ion current at $t=0$ (10^{-9} A)	Electron current (μA)	Storage pressure (Torr)	Electron energy (eV)	$(i_I/i_e P_0)$ (10^{-3} Torr^{-1})	$\sigma_T(E)/[\sigma_T(60)]_{H_2}$	σ_T (calc.) (πa_0^2)	$(\sigma_T)_{EFM}/(\sigma_T)_{MGM}$
1	H_2	1.21	1.00	668	60	1.811	1.00	1.100[a]	...
1	D_2	1.21	1.00	662	60	1.828	1.009	1.110	0.99
1	He	0.459	1.00	687	90	0.668	0.369	0.406	1.04
1	Kr	1.08	1.00	141	60	7.66	4.23	4.65	0.92
1	CO	1.27	0.80	322	90	4.93	2.72	2.99	0.96
1	N_2O	1.46	0.80	307	60	5.95	3.28	3.61	0.90
1	CH_4	1.62	0.80	293	90	6.91	3.82	4.20	0.93
2	H_2	0.698	0.80	458	60	1.906	1.00	1.100[a]	...
2	Ne	0.521	0.80	527	90	1.236	0.648	0.713	1.035
2	N_2	1.40	0.80	358	90	4.89	2.57	2.83	0.91
2	Ar	2.29	0.80	546	60	5.25	2.75	3.02	0.88
2	CO_2	1.255	0.75	290	60	5.77	3.03	3.33	0.94
2	Xe	1.42	0.50	287	60	9.89	5.19	5.71	0.73
3	H_2	0.416	1.00	691	60	0.602	1.00	1.100[a]	...
3	SF_6	0.78	0.70	353	60	3.16	5.25	5.78	...
3	C_2H_4	0.84	0.70	353	60	3.40	5.65	6.22	...

[a] Calculated using the value $[\sigma_T(60)]_{H_2}=1.100\ \pi a_0^2$ from the McLeod-gauge measurements.

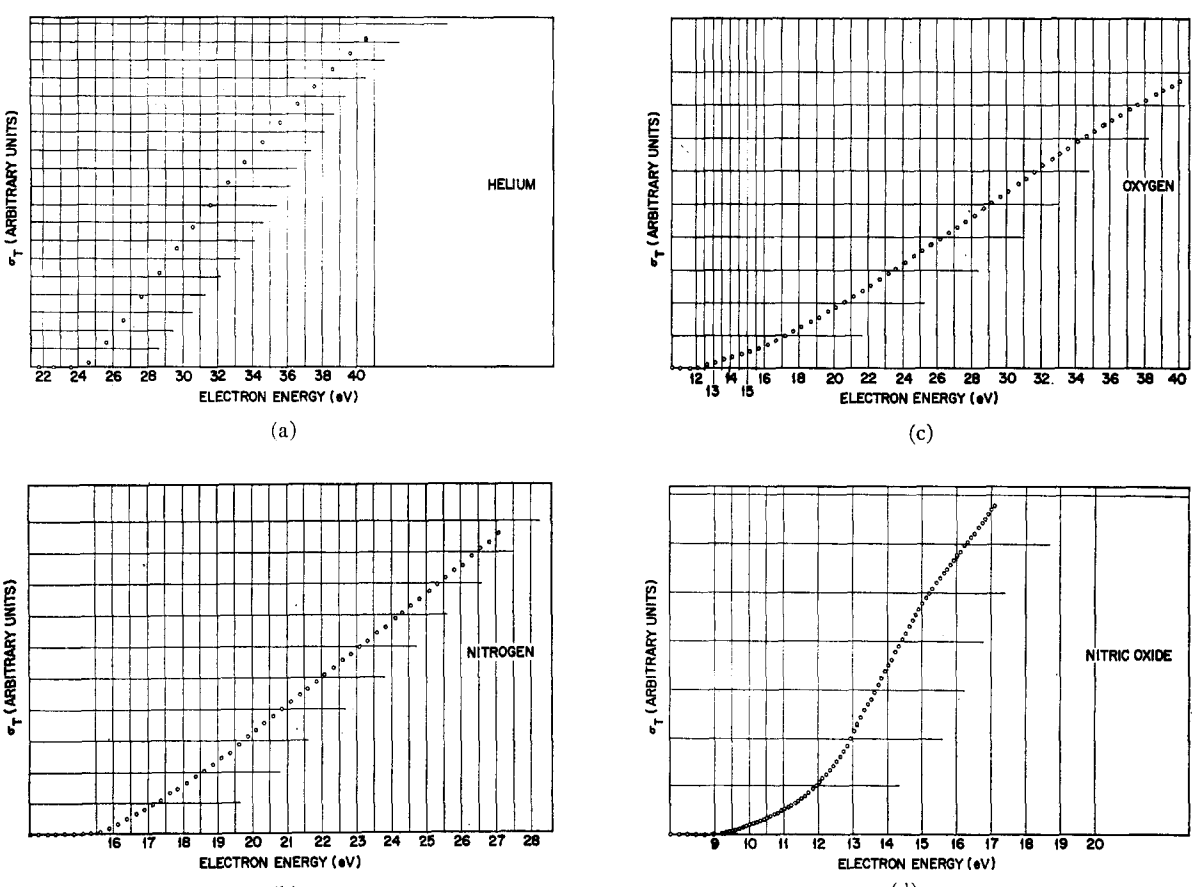

FIG. 4. Original plot of relative cross section for ionization of a gas by electron impact near threshold. (a) Helium, (b) nitrogen, (c) oxygen, (d) nitric oxide.

TABLE V. Experimental total ionization cross sections vs electron energy for the rare gases in units of (πa_0^2). Absolute cross sections are normalized by effusive-flow measurements relative to H_2, which was determined by direct McLeod-gauge measurement.

E (eV)	He	Ne	Ar	Kr	Xe	E (eV)
1000	0.160	0.439	1.04	1.58	2.14	1000
950	0.165	0.452	1.07	1.63	2.21	950
900	0.171	0.470	1.12	1.69	2.29	900
850	0.178	0.485	1.16	1.75	2.38	850
800	0.187	0.505	1.21	1.82	2.48	800
750	0.194	0.526	1.26	1.91	2.59	750
700	0.205	0.550	1.32	2.00	2.71	700
650	0.216	0.576	1.39	2.10	2.83	650
600	0.227	0.600	1.48	2.21	2.98	600
550	0.240	0.638	1.56	2.32	3.14	550
500	0.255	0.667	1.66	2.46	3.35	500
450	0.272	0.700	1.76	2.61	3.56	450
400	0.292	0.714	1.91	2.80	3.81	400
350	0.313	0.780	2.06	3.02	4.09	350
300	0.337	0.821	2.25	3.26	4.43	300
250	0.365	0.860	2.47	3.56	4.80	250
200	0.394	0.888	2.72	3.93	5.21	200
187.5	...	0.890	...	...	...	187.5
180	...	...	2.86	4.10	5.50	180
175	0.408	0.888	...	...	...	175
160	...	...	2.98	4.26	5.76	160
150	0.419	0.878	3.05	4.35	5.90	150
145	0.421	0.867	3.08	4.41	5.97	145
140	0.423	0.860	3.10	4.45	6.01	140
135	0.424	0.850	3.12	4.50	6.08	135
130	0.425	0.844	3.14	4.54	6.16	130
125	0.425	0.836	3.17	4.59	6.18	125
120	0.424	0.824	3.19	4.64	6.20	120
115	0.423	0.810	3.21	4.68	6.21	115
110	0.421	0.796	3.22	4.71	6.20	110
105	0.419	0.778	3.23	4.75	6.16	105
100	0.416	0.758	3.24	4.77	6.12	100
95	0.411	0.738	3.25	4.79	6.06	95
90	0.406	0.714	3.25	4.81	5.99	90
85	0.399	0.687	3.24	4.83	5.97	85
80	0.391	0.656	3.23	4.84	5.89	80
75	0.380	0.622	3.20	4.83	5.84	75
70	0.365	0.584	3.15	4.79	5.82	70
65	0.350	0.542	3.10	4.74	5.78	65
60	0.330	0.495	3.02	4.65	5.72	60
57.5	...	...	2.98	4.58	...	57.5
55	0.308	0.445	2.95	4.51	5.62	55
52.5	...	...	2.91	4.44	...	52.5
50	0.276	0.384	2.88	4.36	5.50	50
47.5	...	...	2.85	4.26	...	47.5
45	0.239	0.321	2.83	4.17	5.32	45
42.5	...	...	2.78	4.07	...	42.5

E (eV)	He	Ne	Ar	Kr	Xe	E (eV)
40	0.195	0.259	2.72	3.97	5.09	40
38	0.176	0.323	2.65	3.85	4.99	38
36	0.154	0.204	2.55	3.71	4.88	36
34	0.130	0.175	2.40	3.56	4.76	34
33.5	0.124	...	...	...	...	33.5
33	0.118	0.161	...	...	...	33
32.5	0.112	...	...	...	...	32.5
32	0.105	0.146	2.23	3.37	4.60	32
31.5	0.0982	0.138	...	...	...	31.5
31	0.0912	0.131	...	...	...	31
30.5	0.0838	0.123	...	...	...	30.5
30	0.0766	0.116	2.05	3.15	4.38	30
29.5	0.0698	0.109	...	...	...	29.5
29	0.0628	0.101	...	...	...	29
28.5	0.0552	0.0938	...	...	...	28.5
28	0.0483	0.0866	1.82	2.87	4.11	28
27.5	0.0413	0.0792	...	...	...	27.5
27	0.0344	0.0718	...	...	...	27
26.5	0.0268	0.0644	...	...	...	26.5
26	0.0199	0.0566	1.60	2.55	3.83	26
25.5	0.0129	0.0498	1.54	...	...	25.5
25	0.0059	0.0432	1.48	...	...	25
24.5	...	0.0365	1.41	...	...	24.5
24		0.0296	1.34	2.19	3.52	24
23.5		0.0230	1.27	2.10	...	23.5
23		0.0166	1.20	2.00	3.33	23
22.5		0.0101	1.13	1.90	3.22	22.5
22		0.0037	1.06	1.80	3.11	22
21.5		...	0.975	1.70	2.98	21.5
21			0.895	1.60	2.83	21
20.5			0.810	1.49	2.71	20.5
20			0.713	1.39	2.59	20
19.5			0.621	1.27	2.46	19.5
19			0.523	1.15	2.33	19
18.5			0.429	1.03	2.19	18.5
18			0.334	0.908	2.05	18
17.5			0.241	0.777	1.90	17.5
17			0.152	0.655	1.74	17
16.5			0.076	0.528	1.57	16.5
16			0.023	0.407	1.40	16
15.5			...	0.290	1.22	15.5
15				0.182	1.03	15
14.5				0.089	0.844	14.5
14				...	0.650	14
13.5					0.469	13.5
13					0.291	13
12.5					0.125	12.5
12					...	12

$\pm 0.5\%$. Usually, the reproducibility was $\sim\pm 0.3\%$. The electron current never changed by more than $\sim 20\%$ over the energy range in a given run, and the linearity of the Keithley 600-A electrometer used for electron current was shown to be excellent over this range. Also, Cary Model 31 electrometer used for ion current was shown to be linear to $\sim 0.2\%$ over the range used. The one remaining question is possible variations in l as a function of electron energy. Massey and Burhop[28] estimated the maximum possible path-length correction by assuming the electrons could pick up large transverse velocity components, and calculating the maximum possible path length for an electron that has enough transverse energy to travel on a helix that just barely passes through the final aperture. They used the formula

$$(l_{\max}/l) = 1 + (1.1 \times 10^{-4} d^2 H^2 / E_0), \qquad (5)$$

where l is the geometric straight-line path length, d is the final aperture diameter in millimeters, H is the magnetic field in gauss, and E_0 is the axial electron energy in electron volts. They did not stipulate where these large transverse velocity components come from, and indeed, as Asundi[29] points out, electrons would have to acquire 32 eV of transverse energy to pass through a helix of diameter 1.5 mm as in the experiment of Tate and Smith.[2] This is hardly possible on several grounds,[29] and Asundi[29] proposes that the actual path-length correction is considerably smaller than

[28] H. S. W. Massey and E. H. S. Burhop, *Electronic and Ionic Impact Phenomena* (Oxford University Press, New York, 1952).

[29] R. K. Asundi, Proc. Phys. Soc. (London) **82**, 372 (1963).

TABLE VI. Experimental total ionization cross sections for diatomic molecules in units of πa_0^2. Absolute cross sections for H_2 were determined directly by means of a McLeod gauge. Absolute normalization of D_2, N_2, and CO was accomplished by the effusive-flow technique. Absolute normalization for O_2 and NO was accomplished by reducing the McLeod-gauge cross sections by 7%.

E (eV)	H_2	D_2	N_2	O_2	CO	NO	E (eV)
1000	0.273	0.281	1.05	1.20	1.09	1.37	1000
950	0.284	0.292	1.09	1.24	1.13	1.41	950
900	0.296	0.308	1.12	1.29	1.17	1.15	900
850	0.308	0.320	1.17	1.34	1.21	1.51	850
800	0.322	0.335	1.21	1.40	1.26	1.58	800
750	0.339	0.352	1.26	1.46	1.31	1.65	750
700	0.358	0.370	1.32	1.53	1.38	1.72	700
650	0.380	0.391	1.40	1.61	1.44	1.81	650
600	0.403	0.416	1.47	1.69	1.53	1.90	600
550	0.430	0.440	1.55	1.80	1.62	2.00	550
500	0.462	0.471	1.65	1.90	1.70	2.11	500
450	0.498	0.507	1.76	2.02	1.81	2.25	450
400	0.541	0.548	1.89	2.14	1.96	2.40	400
350	0.589	0.594	2.02	2.30	2.10	2.58	350
300	0.651	0.655	2.18	2.48	2.26	2.78	300
250	0.723	0.725	2.37	2.68	2.46	3.01	250
200	0.813	0.814	2.58	2.88	2.69	3.25	200
180	0.855	0.857	2.67	2.98	2.78	3.36	180
160	0.898	0.900	2.75	3.03	2.87	3.46	160
150	0.924	0.924	2.79	3.06	2.92	3.50	150
145	0.933	0.940	2.81	3.07	2.93	3.51	145
140	0.944	0.954	2.82	3.080	2.95	3.52	140
135	0.959	0.970	2.83	3.087	2.96	3.53	135
130	0.970	0.984	2.85	3.091	2.98	3.55	130
125	0.982	0.997	2.86	3.096	2.99	3.565	125
120	0.998	1.010	2.870	3.096	3.003	3.573	120
115	1.013	1.031	2.872	3.091	3.009	3.580	115
110	1.026	1.038	2.874	3.084	3.018	3.580	110
105	1.041	1.052	2.872	3.06	3.018	3.577	105
100	1.050	1.067	2.870	3.04	3.012	3.569	100
95	1.062	1.078	2.85	3.01	3.003	3.561	95
90	1.078	1.089	2.83	2.98	2.99	3.54	90
85	1.089	1.100	2.80	2.93	2.96	3.49	85
80	1.096	1.107	2.77	2.86	2.94	3.45	80
75	1.103	1.114	2.72	2.80	2.88	3.38	75
70	1.104	1.115	2.65	2.71	2.84	3.31	70
65	1.104	1.115	2.58	2.60	2.76	3.21	65
60	1.100	1.110	2.48	2.47	2.66	3.11	60
55	1.090	1.100	2.35	2.31	2.55	2.97	55
50	1.070	1.080	2.20	2.14	2.41	2.82	50
45	1.038	1.058	2.02	1.93	2.24	2.62	45
40	0.984	0.996	1.79	1.67	2.03	2.37	40
38	0.955	0.967	1.69	1.55	1.93	2.26	38
36	0.023	0.933	1.57	1.44	1.82	2.13	36
34	0.882	0.894	1.44	1.31	1.70	2.01	34
32	0.837	0.846	1.31	1.17	1.57	1.88	32
30	0.782	0.794	1.17	1.02	1.41	1.73	30
28	0.718	0.729	0.995	0.875	1.24	1.59	28
26	0.640	0.654	0.812	0.744	1.06	1.43	26
25.5	0.618	0.632	0.769	...	...	...	25.5
25	0.596	0.610	0.727	...	...	...	25
24.5	0.574	0.589	0.685	...	...	...	24.5
24	0.550	0.566	0.642	0.608	0.871	1.26	24
23.5	0.524	0.540	0.600	...	0.823	...	23.5
23	0.499	0.516	0.559	...	0.778	...	23
22.5	0.470	0.488	0.517	...	0.731	...	22.5
22	0.443	0.462	0.475	0.473	0.683	1.09	22
21.5	0.412	0.435	0.432	0.440	0.636	...	21.5
21	0.382	0.404	0.391	0.409	0.586	...	21
20.5	0.352	0.373	0.350	0.379	0.537	...	20.5
20	0.318	0.341	0.307	0.349	0.487	0.924	20
19.5	0.283	0.309	0.262	0.317	0.439	0.880	19.5
19	0.250	0.272	0.226	0.288	0.387	0.837	19
18.5	0.213	0.235	0.186	0.260	0.338	0.797	18.5
18	0.177	0.197	0.147	0.231	0.289	0.754	18
17.5	0.140	0.157	0.112	0.205	0.243	0.710	17.5
17	0.105	0.118	0.081	0.180	0.201	0.665	17
16.5	0.069	0.078	0.053	0.155	0.158	0.620	16.5
16	0.034	0.039	0.024	0.130	0.121	0.572	16
15.5	...	...	...	0.112	0.087	0.524	15.5

TABLE VI (*Continued*)

E (eV)	H_2	D_2	N_2	O_2	CO	NO	E (eV)
15				0.097	0.058	0.475	15
14.5				0.078	0.031	0.414	14.5
14				0.061	...	0.347	14
13.5				0.046		0.277	13.5
13				0.026		0.209	13
12.5				0.012		0.149	12.5
12				...		0.105	12
11.5						0.073	11.5
11						0.053	11
10.5						0.035	10.5
10						0.020	10
9.5						0.013	9.5
9						...	9

that given by Massey and Burhop. Asundi[29] calculates the maximum transverse velocity component imparted to the electrons due to the electrostatic lens effect of the accelerating apertures, and finds it to be ~0.001 of the total accelerating voltage. Thus he concludes that path-length corrections in typical total-ionization experiments are small.

In actual practice, even the electrostatic lens effects are completely negligible at high magnetic fields. At several hundred gauss, one reaches the limiting case

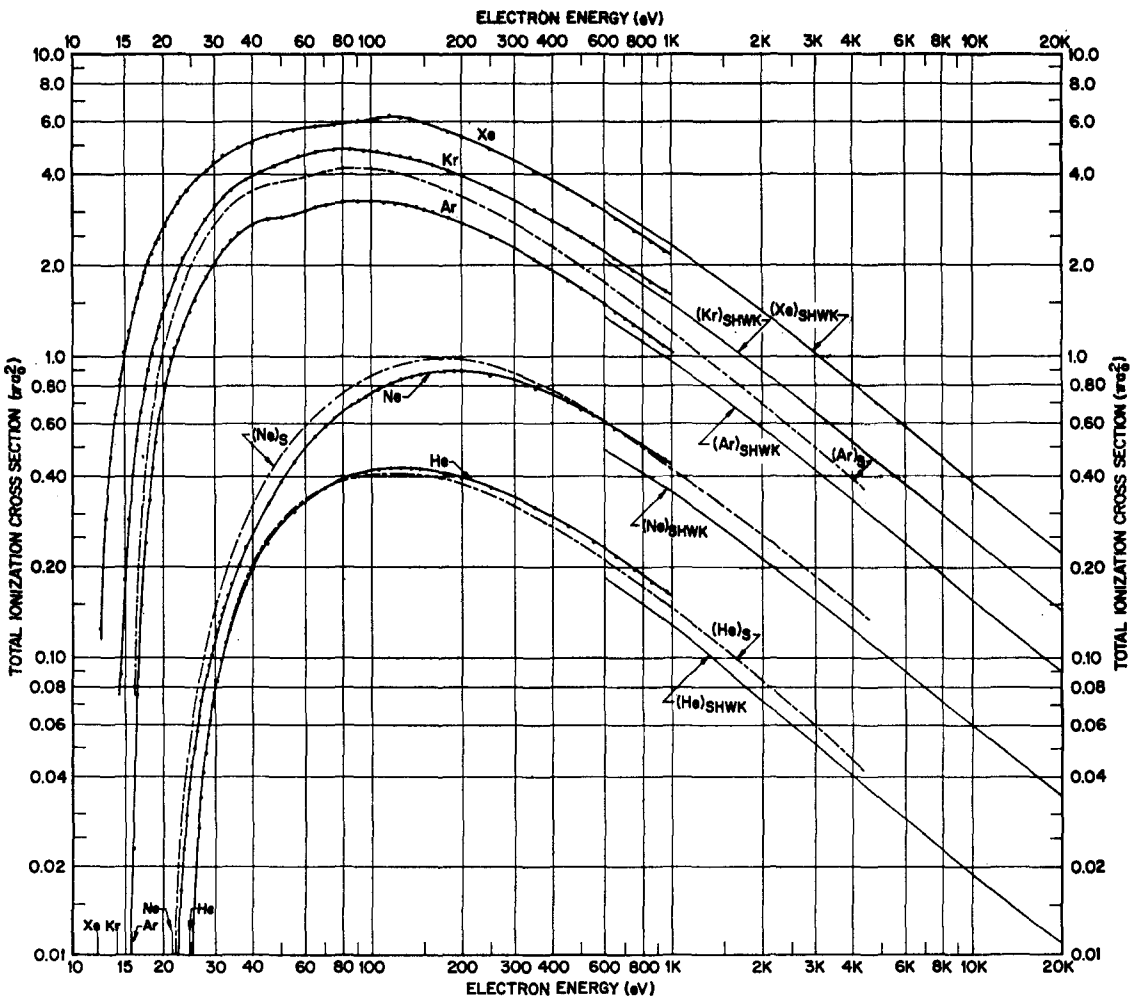

FIG. 5. Comprehensive plot of total ionization cross sections for the rare gases by electron impact from threshold to 20 keV. The data points are from the present work. The lines labeled "SHWK" and "S" are from Schram, de Heer, Van der Wiel, and Kistemaker,[16] and from Smith,[1] respectively.

TABLE VII. Experimental ionization cross sections for polyatomic molecules in πa_0^2. Absolute normalization was accomplished by effusive-flow measurements relative to H_2, which was determined directly by means of a McLeod gauge.

E(eV)	CO_2	N_2O	CH_4	SF_6	C_2H_4	E(eV)
1000	1.59	1.61	1.34			1000
950	1.62	1.65	1.37			950
900	1.67	1.70	1.41			900
850	1.72	1.76	1.46			850
800	1.79	1.85	1.52			800
750	1.88	1.93	1.59			750
700	1.97	2.02	1.67			700
650	2.07	2.12	1.75			650
600	2.17	2.24	1.85			600
550	2.30	2.37	1.95			550
500	2.43	2.53	2.08			500
450	2.58	2.69	2.21			450
400	2.75	2.87	2.38			400
350	2.95	3.09	2.58			350
300	3.19	3.34	2.83	6.92		300
250	3.43	3.61	3.09	7.36		250
200	3.70	3.92	3.42	7.76		200
180	3.82	4.03	3.54	7.68		180
160	3.91	4.14	3.69	7.92		160
150	3.96	4.20	3.78	7.92		150
145	3.99	4.22	3.84	7.89	6.13	145
140	4.00	4.24	3.88	7.88	6.16	140
135	4.02	4.26	3.92	7.86	6.26	135
130	4.03	4.27	3.96	7.82	6.32	130
125	4.034	4.28	4.00	7.81	6.37	125
120	4.040	4.29	4.04	7.79	6.43	120
115	4.040	4.29	4.08	7.72	6.48	115
110	4.030	4.28	4.11	7.63	6.52	110
105	4.01	4.27	4.13	7.53	6.56	105
100	4.00	4.26	4.16	7.42	6.58	100
95	3.97	4.24	4.18	7.30	6.62	95
90	3.93	4.20	4.200	7.14	6.625	90
85	3.88	4.16	4.205	6.98	6.62	85
80	3.81	4.10	4.200	6.76	6.59	80
75	3.72	4.01	4.18	6.56	6.55	75
70	3.61	3.91	4.16	6.42	6.47	70
65	3.49	3.77	4.11	6.07	6.38	65
60	3.33	3.61	4.05	5.78	6.22	60
55	3.14	3.42	3.95	5.47	6.01	55
50	2.94	3.19	3.82	4.94	5.76	50
45	2.69	2.94	3.65	4.31	5.46	45
40	2.40	2.63	3.43	3.94	5.11	40
38	2.27	2.49	3.31	3.70	4.94	38
36	2.15	2.35	3.17	3.46	4.75	36
34	2.02	2.21	3.05	3.07	4.52	34
32	1.88	2.05	2.89	2.62	4.27	32
30	1.72	1.86	2.70	2.19	4.00	30
28	1.52	1.67	2.50	1.77	3.69	28
26	1.27	1.46	2.24	1.43	3.35	26
24	1.00	1.22	1.96	0.932	2.77	24
23.5	0.941	1.15	1.88	0.816	2.67	23.5
23	0.883	1.09	1.79	0.706	2.58	23
22.5	0.826	1.02	1.70	0.610	2.48	22.5
22	0.768	0.954	1.61	0.520	2.38	22
21.5	0.708	0.887	1.52	0.445	2.27	21.5
21	0.656	0.822	1.41	0.376	2.16	21
19.5	0.514	0.626	1.11	0.220	1.81	19.5
19	0.486	0.564	1.00	0.176	1.69	19
18.5	0.424	0.512	0.901	0.134	1.56	18.5
18	0.379	0.459	0.802	0.095	1.44	18
17.5	0.333	0.411	0.693	0.063	1.32	17.5
17	0.290	0.363	0.603	0.040	1.20	17
16.5	0.244	0.318	0.506	0.023	1.09	16.5
16	0.198	0.271	0.410		0.978	16
15.5	0.154	0.226	0.316		0.854	15.5
15	0.110	0.180	0.225		0.729	15
14.5	0.063	0.137	0.148		0.606	14.5
14	...	0.061	0.084		0.490	14
13.5		...	0.039		0.392	13.5
13			...		0.299	13
12.5					0.219	12.5
12					0.152	12
11.5					0.099	11.5
11					0.051	11
10.5					0.013	10.5

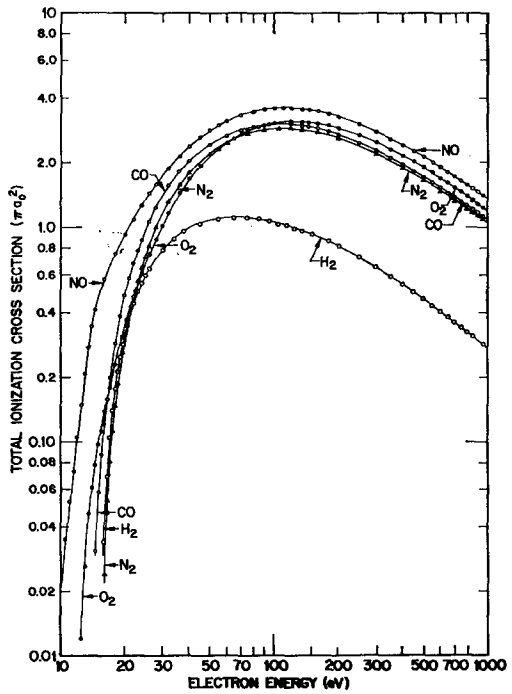

FIG. 6. Comprehensive plot of total ionization cross sections for diatomic molecules by electron impact from threshold to 1000 eV, as determined in the present experiment.

of confined flow, in which the electron trajectories are straight lines from cathode to electron collector.[30] In our experiments, at 500–600 G, there are essentially no transverse velocity components due to electrostatic forces to create path-length corrections. Thus *in vacuo*, the path-length correction is totally negligible, and the electron trajectories are essentially straight lines.

However, in the presence of a gas, elastic and inelastic scattering of electrons by the gas can create a broad distribution of transverse velocities. This source of transverse energy is not necessarily negligible at the pressures encountered in some total ionization tubes. Equation (5) can be rewritten as

$$l_{\max}/l = 1 + 0.92 E_\perp/E_0, \qquad (6)$$

in which d is now taken as the diameter corresponding to the circular motion of an electron with energy $E_\perp$ transverse to magnetic field H. One can see that although the correction predicted in Eq. (5) is proportional to the square of the magnetic field, the correction predicted in Eq. (6) is independent of magnetic field. Both in our experiments, and in that of Smith,[8] the observed ionization cross section is independent of magnetic field at high fields. Thus the problem of the path-length correction is entirely dependent on elastic scattering as a source of transverse velocity, and independent of electrostatic defocusing effects. To estimate path-length corrections from elastic scattering, we chose the example of H_2, for which the total cross section for electron scattering[31] is $\cong 6\times10^{-16}$ cm^2 near the ionization threshold (15.4 eV) Since the path distance from vacuum separating electrode to the ionization chamber is $\cong 5$ cm, σl for elastic scattering is $\cong 3\times10^{-15}$ cm^3. The average angular scattering deviation is not known exactly, but let us assume for purposes of argument that it is 30°. Thus the average transverse energy pickup per collision is $\cong E_0 \sin^2 30° = E_0/4$. But the number density at a pressure of $\cong 5\times10^{-5}$ Torr is $\cong 2\times10^{12}$ particle/cc. Then the probability of an electron-scattering event between the cathode and the ionization chamber is $\sigma n l \cong 0.006$, and the average $E_\perp$ for these collisions is $\cong E_0/4$. Thus, near ionization threshold, the average path-length correction due to scattering is $(l_{\max}-l)/l = 0.92\ E_\perp/E_0 \cong 0.23$ for about 0.6% of the electron current. The net average path-length correction for the entire electron beam is $\cong 0.006\times0.23 = 0.0014$, or 0.14%. At higher electron energies, the scattering cross section decreases, and the scattering becomes more peaked in the forward direction, thus further reducing the path-length correction. We may therefore conclude that path-length corrections were small in the experiments reported herein and that l may be taken as the geometric path length. It is important to have the magnetic field high enough to be in the region of confined flow, or scalloping[30] can produce large electrostatic path-length corrections. In our work, a minimum of 300 G was necessary to make the ionization cross sections independent of electron energy at low electron energies.

The accuracy of plotting and reading the actual data for i_I/i_e vs E_0 was better than $\pm0.5\%$ Thus, it is believed that the energy dependence of the total ionization cross sections measured in the present work is accurate to better than $\pm1\%$, except that above 800 eV the complete collection of the electron current was subject to minor fluctuations, and the accuracy of the relative cross sections is probably $\sim\pm2\%$. Over limited ranges of electron energy, as for example near the maxima in the cross sections, great care was taken to assure that the accuracy of plotting and constancy of pressure was very reliable. The accuracy of the relative cross sections for such limited energy ranges is probably $\pm0.3\%$.

The absolute normalization of the cross sections is subject to considerably more doubt. The absolute cross section in H_2 was determined by using a McLeod gauge to determine the gas pressure. Although great care was taken in the readings to avoid sticking of the mercury columns in the capillaries, it is very difficult to assess possible errors due to this effect. It is presumed that errors due to deviations from free molecular flow and pumping action of the mercury stream are negligible. The accuracy of pressure measurement for H_2 is estimated to be $\pm3\%$. The ion-current electrometer was

[30] J. R. Pierce, *Theory and Design of Electron Beams* (D. Van Nostrand Company, Inc., New York, 1954), 2nd ed.

[31] J. B. Hasted, *Physics of Atomic Collisions* (Butterworths Scientific Publications, Ltd., London, 1964), pp. 169–173.

calibrated to within ±0.5%, and the electron-current electrometer to within ±0.7% by means of standard voltage sources and resistors. The temperature and path-length measurements were accurate to ±0.3%. The estimated maximum possible error in the absolute normalization in H_2 is ±4.5%.

The absolute normalization of gases other than H_2, O_2, and NO was achieved by means of the effusive-flow technique described in Appendix 1. The accuracy of these results depends on the linearity of the electrometers (better than ±0.2%), the accuracy of measurement of P_0 (Wallace & Tiernan gauge rated at ±0.3% by manufacturer), constancy of the leak-valve opening, and the adequacy of the assumption of effusive flow. The tests for effusive flow were satisfactory, as shown in Table IV, but it was difficult to carry out these measurements to a very high precision. The only test of the constancy of the leak-valve opening was to study H_2 before and after the other gases were studied and find no change in the current-vs-time characteristic. This was found to be the case to within the precision possible in these runs. It is estimated that the accuracy of the cross sections of gases relative to H_2 is probably somewhat better than the initial measurement in H_2, so that the maximum possible error in normalization of gases other than H_2, O_2, and NO is probably ~±7%. The accuracy of absolute normalization of O_2 and NO is difficult to assess (see Appendix), and may possibly be ±10%.

The available data on total ionization cross sections are summarized in Ref. 20. There are essentially four main groups that have investigated total ionization cross sections; those of Refs. 1 and 2, Ref. 16, Refs. 17 and 18, and the present work. We refer to these groups as TS, SHWK, and ACK, respectively. In the work of TS and ACK, no corrections were made to direct McLeod-gauge readings of gas pressure. It is not clear whether correction was made by ACK for thermal transpiration as in Eq. (3). In the work by SHWK, correction to McLeod-gauge measurements was made by cooling the neck of the McLeod gauge as suggested by Ishii and Nakayama.[27] This procedure may help in reducing errors due to deviations from free molecular flow in the tube connecting the McLeod gauge to the cold trap, by increasing the mean free path of gas due to the absence of mercury. The explanation given by Ishii and Nakayama in terms of pumping action of the mercury may be a gross oversimplification.[32] In all cases, great care was apparently taken in carrying out the experiments. Consistency checks such as complete collection of electrons and ions are discussed extensively by TS, but not very much by ACK. The ion saturation curves presented by SHWK show remarkably large ion currents shot back into the ionization region of the gun from their electron-collector region. Their "collimator" appears to be a strong source of secondary electrons, and may cause disturbing path-length effects. Also, their background pressure of 5×10^{-6} Torr in the ionization region leads to gas purities of only 98% at operating pressures of $\sim2\times10^{-4}$ Torr.

[32] D. D. Briglia (personal communication).

TABLE VIII. Comparison of total ionization cross sections of various investigators below 100 eV.

Gas	E eV	$\sigma_T(\pi a_0^2)$ This work	$\sigma_T(\pi a_0^2)$ ACK	$\sigma_T(\pi a_0^2)$ TS
He	40	0.195	0.199	0.204
He	90	0.406	0.431	0.392
Ne	40	0.259	0.281	0.322
Ne	90	0.714	0.821	0.810
Ar	40	2.72	3.32	3.51
Ar	90	3.25	4.02	4.18
Kr	40	3.97	5.26	...
Kr	90	4.81	6.31	...
Xe	40	5.09	7.31	...
Xe	90	5.99	8.80	...

A comparison of the data of the present work with data of SHWK and TS is given in Fig. (5). Unfortunately, the data of ACK could not be included without greatly confusing the diagram. The data of ACK are from threshold to 100 eV, and are compared with other investigators at several selected energies in Table VIII.

In general, the energy dependence of the cross sections measured in the present work are in good agreement with the cross sections measured by SHWK from 600 eV to 20 keV. However, the absolute magnitudes are not in good agreement, the work of SHWK tending to be less than ours by ~8% in Ar and Kr, and by ~20% in He and Ne, and exceeding ours by ~8% in Xe. The cross sections of ACK generally exceed ours by amounts ranging up to 50%. The energy dependences of the cross sections are not in such bad agreement. There seems to be a systematic tendency for the results of TS to approach ours at high electron energy, and to exceed ours more and more toward threshold.

In the diatomic molecules, our results again tend to exceed the cross sections of SHWK by about 20%, and the results of TS tend to exceed ours by about 15%. The results of ACK parallel those of TS.

It is difficult to explain these differences. It appears that the ratio of observed cross sections relative to that of H_2 obtained by SHWK is in fair agreement in most cases with the present work. That is, the discrepancy in most cases (Xe is a single exception) is greatly reduced between our work and that of SHWK, if the SHWK cross sections is multiplied by ~1.2 or if our cross sections are divided by ~1.2. McLeod-gauge errors[27] may account for most of the differences in magnitude found between cross sections measured by various investigators. It is difficult to see why the energy dependences of the cross sections measured by TS are not closer to ours. They measured their relative cross sections at considerably higher pressures (~factor

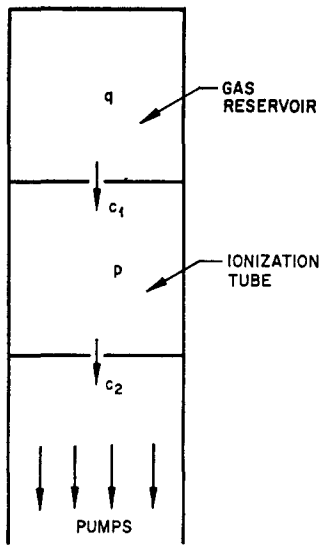

FIG. 7. Simplified flow diagram for effusive-flow technique for measuring ionization cross sections of gases relative to H_2. Chamber q, originally at pressure Q, is opened to Chamber p, originally at zero pressure, at time $t=0$. The conductances of the small holes leading from q to p, and from p to the pumps, are c_1 and c_2, respectively.

of 10) than we did, and may possibly have had slight path-length corrections.

ACKNOWLEDGMENTS

The authors would like to acknowledge the contributions of a number of assistants and associates during the course of this work. Mr. M. Green did important preliminary research on vacuum systems and oxide-coated cathodes. Dr. D. D. Briglia provided capable advice on many aspects of the work, especially the data-recording system. Dr. Terry E. Sharp supplied important advice in connection with the preparation of the Appendix to this paper. We wish to thank Dr. L. J. Kieffer for reading the manuscript and pointing out several errors. The support of the Lockheed Independent Research Program is gratefully acknowledged.

APPENDIX. A METHOD FOR DETERMINING IONIZATION CROSS SECTIONS OF GASES RELATIVE TO THE IONIZATION CROSS SECTION OF H_2

If the absolute total cross section for ionization of H_2 has been determined from McLeod-gauge measurements, one need only devise a method for relating the cross sections of other gases to that of H_2. This appendix describes a method for doing this by means of an effusive-flow technique.

In this method, a finite gas reservoir supplies gas to the ionization tube through a leak valve. If the supply pressure is maintained sufficiently low so that the mean free path is long compared to the critical dimension in the opening of the leak valve, the flow through the leak valve will be effusive. In this case, the volumetric conductance of gas through the leak valve c_1 will be inversely proportional to the molecular weight of the gas. The flow of gas from the ionization tube through the small hole (area $\cong 2\times 10^{-4}$ in.^{2}) connecting it to the pumps[19,21,22] is certainly effusive, so that the conductance through this hole is also inversely proportional to the molecular weight of the gas. It can then be shown that the quasi steady-state pressure in the ionization tube resulting from connecting a gas reservoir to a preset leak valve, is proportional to the reservoir pressure, and *independent of molecular weight*. Thus, the relative total ionization cross sections for a series of gases can be determined by passing them through a preset leak valve from a reservoir of known pressure.

The theory of the method is as follows. Two chambers are connected in series by small apertures to a pump, as shown in Fig. 7. At $t=0$, the pressure in the reservoir, q, is equal to Q, and the pressure in the ionization tube, p, is zero. The time rates of change of pressure in the compartments are

$$V_p(dp/dt) = -c_2p+c_1q,$$
$$V_q(dq/dt) = -c_1q, \tag{A1}$$

where V_p and V_q are the volumes of the ionization tube and the reservoir, respectively. Denoting $\kappa_1 = c_1/V_q$, $\kappa_2 = c_2/V_p$, and $\kappa_3 = c_1/V_p$, the solutions of these equations are simply

$$q = Q\exp(-\kappa_1 t),$$
$$p = [\kappa_3 Q/(\kappa_2-\kappa_1)][\exp(-\kappa_1 t)-\exp(-\kappa_2 t)]. \tag{A2}$$

When a quasisteady state is reached, $dp/dt \approx 0$, and $p_{SS}(t) = (c_1/c_2)q = (c_1/c_2)Q\exp(-\kappa_1 t)$. In our experiments $(c_1/c_2)\approx 0.004$, and $V_p \approx V_q$. Thus, it is justifiable to neglect κ_1 compared to κ_2 in the second of Eqs. (A2), and obtain

$$p \cong (c_1/c_2)Q[\exp(-\kappa_1 t)-\exp(-\kappa_2 t)]. \tag{A3}$$

We thus see that

$$p(t) \cong p_{SS}(t)[1-\exp(-\kappa_2 t)]. \tag{A4}$$

The theoretical form for the variation of $p(t)$ with t is shown in Fig. 8. The initial buildup of pressure in the ionization tube is almost entirely dependent on c_2, whereas the quasi steady-state pressure decrease is due entirely to c_1. If such plots for several gases were prepared, they should all superimpose if plotted vs $t/M^{\frac{1}{2}}$ on the abscissa, provided one has free molecular flow in c_1 and c_2. Now, if a series of gases are passed through a preset leak valve constituting c_1, and the observed ion currents extrapolated back to zero time as in Fig. 8, the ion currents so determined will be proportional to the ionization cross section σ_T, and the initial reservoir

pressure Q, of each gas. There will be no mass-dependent transmission factors.

The apparatus for performance of this work is outlined in Fig. 9. The bypass valve is closed, and the total ionization tube is evacuated through a small hole in the second aperture plate facing the cathode. The gas reservoir, volume V_4, can be pumped out to $\sim 1\times10^{-8}$ Torr by its own completely separate ultra-high-vacuum system. A preset leak valve connects the reservoir to the ionization tube. The reservoir V_4 is filled by first filling volumes V_1 and V_2 to some initial pressure P_0 ($\sim$500 Torr) that is measured to within 0.3% on an accurately calibrated Bourdon gauge. A small volume of this gas, V_3, is expanded into V_4 to fill the reservoir. Since the ratio $V_4/V_3=4970$, V_4 is filled to 10^{-1} Torr for each 497 Torr in V_3. At the same time that Valve 5 is opened to admit gas from V_3 to V_4, a time sweep is turned on to record ion current in the total ionization tube for a preset electron energy and electron current. The time constants of the system were such as to require about 1.5 min in H_2, and about 13 min in Xe, for the quasisteady state to be reached. Typical traces of ion current vs time are shown in Figs. 10 and 11 for D_2 and CO. It can be seen that they have the same general form as the model shown in Fig. 8. There is a slight delay time in the heavier gases near $t=0$ corresponding to the time required for the gas to expand from V_3 into V_4. In a heavy gas like Xe, this process alone takes about 1.5 min. To test the

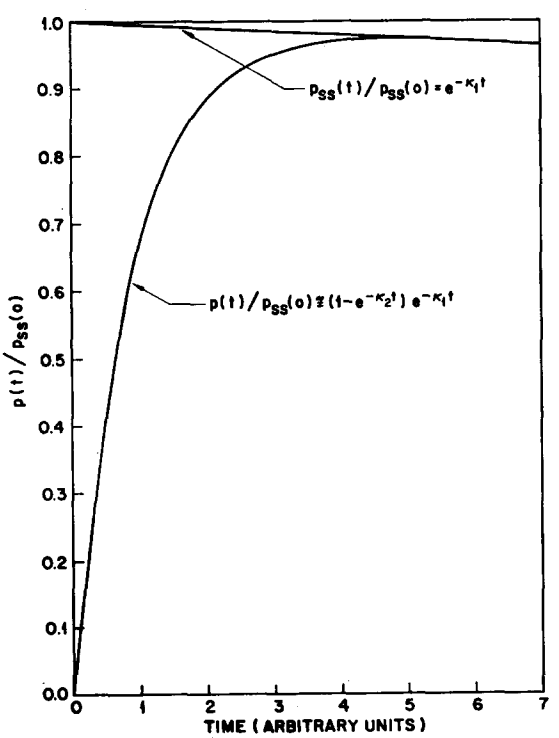

FIG. 8. Plot of the pressure in the ionization tube as a function of time according to Eq. (1.4) under typical operating conditions for H_2.

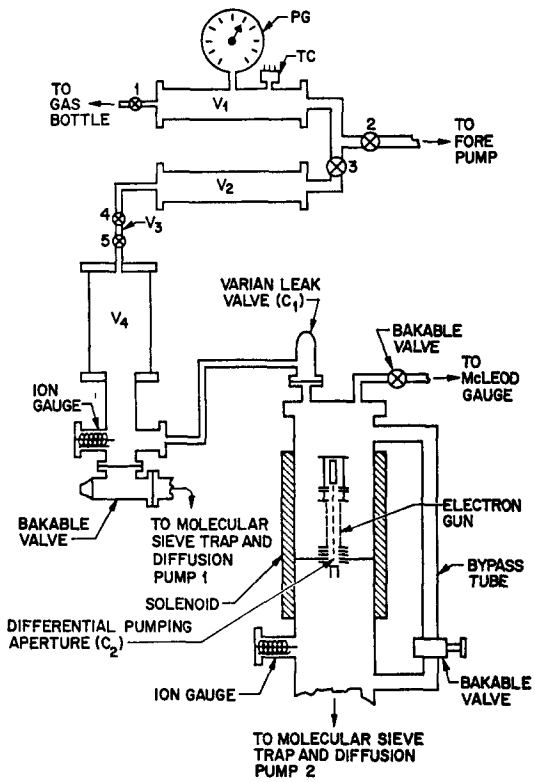

FIG. 9. Detailed apparatus for effusive-flow technique for normalization of ionization cross sections relative to H_2. Gas is stored in volumes V_1 and V_2 (which can be used for accurately blending gas mixtures) at a pressure P_0 which is accurately measured on the Wallace & Tiernan gauge PG. The small volume V_3 of gas at P_0 can be expanded into V_4 ($V_4/V_3=4970$) with the leak valve preset, to start recording of ion current in the ionization tube vs time. The volume V_4 can be pumped down to $\sim 1\times10^{-8}$ Torr by its own separate pumping system. The leak valve constitutes c_1 in Fig. 7 and the small aperture in the second plate of the electron gun above the cathode constitutes c_2. The pumping speed of the pump below the cathode is very large compared to c_2.

validity of the assumption of free molecular flow through c_2, a composite plot of $\ln\{[i_{ss}(t)-i(t)]/i_{ss}(0)\}$ vs t for a number of gases with a fixed leak valve setting is shown in Fig. 12. According to Eqs. (A4), for $c_2 \gg c_1$,

$$[p(t)-p_{ss}(t)]/p_{ss}(0)\cong\exp(-c_2t), \qquad \text{(A5)}$$

and the curves in Fig. 12 should be straight lines with slope $-c_2=-k_2/M^{\frac{1}{2}}$. Table IX shows the ratios of experimentally measured slopes to that of H_2 compared with theory for free molecular flow. The agreement is satisfactory.

The absolute pressures in V_4 in these experiments ranged from about 0.04 Torr for heavy gases to about 0.15 Torr for light gases. The effective area of the opening in the leak valve may be calculated from the observed ratio $c_1/c_2\cong0.004$, and the known effective area of c_2 is 2×10^{-4} in.^{2}. It turns out that the effective diameter of the hole in c_1 is 0.001 in., and the average mean free path of the gas in the pressure range used

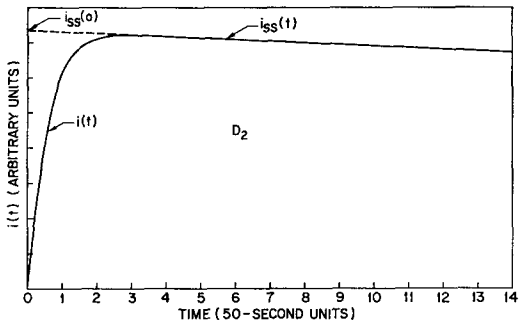

FIG. 10. Ion current in D_2 vs time after expanding gas from V_3 to V_4 with the leak valve preset.

is 0.04 in. in V_4. Thus, one expects the criteria for free molecular flow to be satisfied in the leak valve as well as in the oriface c_2. To directly test the assumption that c_1 is inversely proportional to $M^{\frac{1}{2}}$, one could compare slopes of the steady-state currents at large times. However, in practice, the slopes are sufficiently small that it is impossible to do this with reasonable accuracy. Instead, we have used the fact that the time τ corresponding to the maximum current is given by $\tau = [\ln(\kappa_2/\kappa_1)]/(\kappa_2-\kappa_1)$. Since κ_2 is known to be proportional to $M^{-\frac{1}{2}}$, we find τ proportional to $M^{\frac{1}{2}}$ if κ_1 is also proportional to $M^{-\frac{1}{2}}$. Table IX shows the experimental values for τ/τ_{H_2} for various gases. Insofar as these values agree with $(M/2)^{\frac{1}{2}}$, the validity of the assumption of effusive flow through c_1 is substantiated.

Several series of runs were made for gases passing through a preset leak valve. The ion current was extrapolated to zero time, and the ratio of σ_T for each gas relative to that of H_2 was computed from :

$$\frac{\sigma_T(E)}{[\sigma_T(60)]_{H_2}} = \frac{i_{SS}(0)}{[i_{SS}(0)]_{H_2}} \frac{(i_e)_{H_2}}{i_e} \frac{(P_0)_{H_2}}{P_0}. \quad \text{(A6)}$$

The results are presented in Table IV. For each series of runs, the ratio of i_I/i_eP_0 for each gas to that of H_2 was taken as the ratio of total ionization cross sections. Repeat runs were made for each gas to ensure the accuracy. It was found that reproducibility was better than $\pm 1\%$. The absolute cross section for H_2 was determined by means of McLeod-gauge measurements, and use was made of the free molecular-flow formula, Eq. (3), to correct for thermal transpiration. The result of this work turned out to lead to the value $[\sigma_T(60)]_{H_2} = 1.100\ \pi a_0^2$. This value was used to obtain absolute cross sections for other gases. For the other gases, the ratio of total ionization cross section from

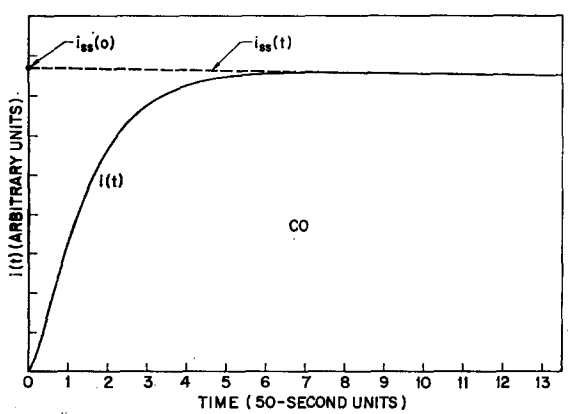

FIG. 11. Ion current in CO vs time after expanding gas from V_3 to V_4 with the leak valve preset.

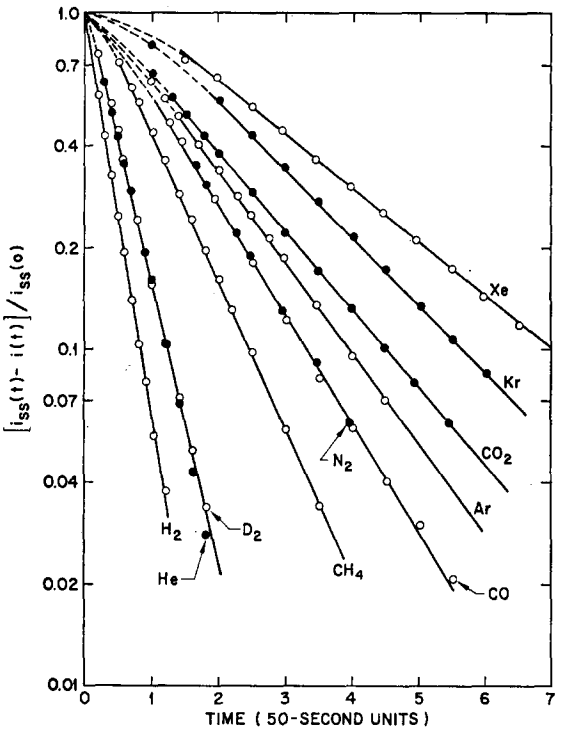

FIG. 12. Composite plot of log $\{[i_{SS}(t) - i(t)]/i_{SS}(0)\}$ vs time for a number of gases with a fixed leak valve setting. According to Eq. (A.5) these plots should be straight lines with slopes proportional to $M^{-\frac{1}{2}}$. Table IX gives the slopes taken from this figure. It should be noted that in the heavier gases, the expansion of gas from V_3 to V_4 requires enough time to cause deviations from linearity over the initial time period.

TABLE IX. Experimental tests of the validity of the assumption of effusive flow through orifices c_1 and c_2.

Gas	Mass	Test for c_2 (slope H_2/slope M)[a]	$(M/2)^{\frac{1}{2}}$	Test for c_1 (τ/τ_{H_2})
H_2	2	1.00	...	1.0
D_2, He	4	1.44	1.41	1.4
CH_4	16	2.79	2.83	2.8
CO	28	3.74	3.74	3.7
Kr	80	6.02	6.32	6.2
N_2	28	3.65	3.74	3.7
CO_2	44	5.14	4.70	4.5
Xe	131	7.60	8.10	7.8
Ar	40	4.55	4.47	4.4

[a] See Figs. 1-6.

effusive-flow measurements, $(\sigma_T)_{EFM}$, to the cross section from direct McLeod-gauge measurement $(\sigma_T)_{MGM}$ is also given for reference. The direct data for McLeod-gauge normalization are summarized in Table II. The cross sections calculated from these measurements are given in Table III. A comparison of the cross sections normalized by means of effusive-flow measurements and those normalized by direct McLeod-gauge measurement is given in the final column of Table IV. It appears that the McLeod-gauge measurements were subject to considerable error in most cases. The cross sections for D_2 are in substantial agreement by both methods. In He and Ne, surprisingly, the McLeod-gauge error was such as to produce apparently low cross sections. In most of the other gases tested, the cross sections normalized by direct McLeod-gauge measurement were too high by 4%–10%. In Xe, the cross section normalized by direct McLeod-gauge measurement was 27% high. Since the random errors of measurement in both McLeod-gauge normalization and in effusive-flow normalization add up to at least $\pm 4\%$, it may be concluded that small differences between $(\sigma_T)_{EFM}/(\sigma_T)_{MGM}$ for similar substances (i.e., CO and N_2) are probably attributable to this cause. The observed results for He and Ne may also be due to this. However, there is little doubt that the heavier gases, on the average, have a higher error than lighter gases, and that Xe has a singularly large McLeod-gauge error. The exact reason for these errors is not clear to the author at this time. The theoretical treatments presented in some of Refs. 27 are far from satisfactory, and further work is being done on this subject in this laboratory.

As a final check on the calibration of cross sections for other gases against that of H_2, the "total-collection mass-spectrometer" method described in Appendix 2 of Ref. 21 was applied to a Ne–H_2 mixture. The Ne–H_2 mixture was accurately blended in the mixing chambers V_1 and V_2 of Fig. 9. It was then run through the system in the usual way, and a plot of ion current vs ion drawout field taken in the usual way.[21] The mixture was 23.2% H_2 and 76.8% Ne, and 60-eV electrons were used. A curve very similar in form to that shown in Fig. 2 of Appendix 2 of Ref. 21 was obtained, giving the separate absolute ion currents for complete collection of Ne ions and all ions. By correcting these currents to zero time, subtracting, and taking the ratio, the ratio of σ_T for Ne to σ_T for H_2 at 60 eV was obtained. Using the relative cross sections for Ne at 60 and 90 eV (see body of this paper), the ratio of $[\sigma_T(90)]_{Ne}/[\sigma_T(60)]_{H_2}$ was determined to be 0.641, which is in good agreement with the value 0.648 given in Table IV.

There were two cases (O_2 and NO) for which it was impossible to normalize the absolute ionization cross section by means of effusive-flow measurements. For these gases it was apparent that chemical effects were taking place on metal surfaces in the ionization tube and in the leak valve. The time required for pumpout after these gases are introduced into a system is unusually long compared to the other gases that have been used. When the effusive-flow technique was applied to these gases, it was found that the quasi-steady state was not reached in 15 min, probably due to "plugging" of the leak-valve opening. The results could not be interpreted in terms of the simple discussion given in this appendix. It was finally decided to roughly estimate the absolute cross sections in these gases by simply reducing the cross sections normalized by direct McLeod-gauge measurements by the average correction factor for other gases of similar mass, namely 7%.